Available online at www.sciencedirect.com

SCIENCE DIRECT®

International Journal of Heat and Mass Transfer 47 (2004) 4821–4832

International Journal of HEAT and MASS TRANSFER

www.elsevier.com/locate/ijhmt

Controlled interface acceleration in unidirectional solidification

R. Xu [a], G.F. Naterer [b,*]

[a] Chalk River Laboratories, AECL, Chalk River, Ontario, Canada K0J 1J0

[b] Department of Mechanical and Manufacturing Engineering, University of Manitoba, 15 Gillson Street, Winnipeg, Manitoba, Canada R3T 2N2

Received 20 March 2004; received in revised form 30 April 2004

Abstract

This paper develops a new experimental/numerical technique for controlling phase interface motion, acceleration and temperature gradients during pure material solidification. The required time-dependent boundary conditions are predicted with an inverse numerical method, in order to produce the desired interfacial motion. The experimental study with freezing of water is performed in a rectangular test cell. Three cases of different interface accelerations are considered. It was observed that an accelerating interface required higher interfacial temperature gradients over time, while these gradients become nearly constant when the phase interface moves at a uniform velocity (zero acceleration). It is noted how the interfacial acceleration and temperature gradients affect the structural characteristics of the solidified microstructures.

1. Introduction

Many technological processes involve solidification, including casting, injection molding, extruding, aircraft icing and phase change materials. During this phase transition, the latent heat of fusion is released at the solid/liquid interface. This thermal energy is transported to the boundaries through the solidified layers along the wall. The interfacial velocity, acceleration and temperature gradient become functions of time, when different time-dependent boundary conditions are applied at the wall. Nucleated crystals may initially appear in the bulk liquid, but this article considers conditions leading to solidification initiated along a stationary wall. During solidification, the interfacial microstructures are largely affected by the interface velocity and temperature gradients on the liquid and solid sides of the interface [1]. These factors have a significant role in the mechanical and thermophysical properties of the solidified material. By effectively controlling the interfacial acceleration, as well as interfacial temperature gradients during solidification, it is considered that a desired material structure with specified properties and material quality can be achieved.

Several past studies have been reported with numerical simulations of solid/liquid phase change [2–5]. However, previous literature regarding experimental studies with deterministic inverse control is relatively limited. Demirci et al. [6] outlined a neural network-based intelligent control, which was successfully applied to molding processes. The control strategy was developed so that a desired flow progression scheme can be specified, while the controller takes corrective actions during the molding process. The control algorithm can be classified as non-deterministic. Non-deterministic methods include conventional control algorithms, such as PID control and neural networks.

A recent experimental study with temperature measurements during directional solidification of metals was presented by Alkemper et al. [7]. The non-deterministic method provided better control of the solidification

* Corresponding author. Tel.: +1-204-474-9805; fax: +1-204-275-7507.

E-mail address: natererg@cc.umanitoba.ca (G.F. Naterer).

0017-9310/$ - see front matter © 2004 Elsevier Ltd. All rights reserved.
doi:10.1016/j.ijheatmasstransfer.2004.04.019

Nomenclature

a	acceleration (m/s^2)
c	specific heat (J/kg K)
e	internal energy (J/kg)
k	thermal conductivity (W/m K)
L	latent heat of phase change (J/kg)
Ste	Stefan number ($c_p\Delta T/L$)
T	temperature (K)
t	time (s)
y	phase interface position (m)

Subscripts

l	liquid
r	reference
s	solid

process, due to direct optical tracking of the solidification process. The design allows an operator to independently select values for the velocity of the solid/liquid interface during solidification, interface acceleration and the temperature gradient on the liquid side of the phase interface. However, the drawback of non-deterministic methods is that they are not based on a physical solution of the governing equations. A non-deterministic algorithm can only be applied with confidence to certain problems, while processes in new problems or new geometries are generally unknown.

In contrast, deterministic methods are based on numerical solutions of the governing equations of solid/liquid phase change [8]. Unlike pure materials such as water, certain dendritic, columnar and other microstructures are found during solidification of alloys [9]. In addition to the energy equation, it has been shown that entropy and the Second Law have significance in solidification modeling [10,11]. Melting in a horizontal tube was reported by Ho and Viskanta [12]. These past studies have generally entailed direct problems, whereby certain boundary conditions are specified and the resulting interior temperatures are calculated.

Unlike these methods, this article extends past studies [13–15] and develops a numerical inverse method for purposes of deterministic control of a solidification process. The method is a combined experimental/numerical control algorithm, which allows temperature gradients at the phase interface to be manipulated for varying interfacial accelerations during solidification of a pure material. The inverse scheme is developed with a Control Volume Based Finite Element Method (CVFEM). This CVFEM predicts the required boundary temperatures to provide a specified interfacial motion during solidification.

In this article, solidification experiments are performed for three cases with different interfacial accelerations in a rectangular test cell. A group of thermocouples was inserted uniformly in the test cell to measure variations of temperature over time. A LabVIEW program analyzed these temperature measurements and saved the results in a data file. The bottom wall temperature was adjusted based on the inverse numerical simulation, by circulating liquid through a heat exchanger. The LabVIEW program was used for communication between the computer and temperature bath. Results are presented and discussed for cases involving a constant cooling temperature, constant velocity and constant acceleration of the interface.

2. Problem formulation

Solidification of a pure material involves a moving phase interface with different thermophysical properties on each side of the interface. The interfacial morphology and microstructure of the solidified material are largely affected by the interfacial velocity, acceleration and temperature gradient. Fig. 1 graphically summarizes a range of interface structures during solidification [1]. It depicts the change of phase interface velocity, V (mm/s), at varying interfacial temperature gradients, $G = \partial T/\partial x$ (K/mm). During a solidification process, varying interfacial velocities and temperature gradients lead to different microstructures, including planar, cellular, dendritic or equiaxed dendritic microstructures. Under certain conditions, nucleation kinetics and other factors affect the solidification process. Also, time-dependent boundary cooling is a major factor affecting the growth of the solidified layer at a wall. This section considers boundary cooling as a predominant factor in controlling interfacial motion and temperature gradients, thereby affecting the microstructure development.

Consider solidification in a rectangular test cell (see Fig. 2) occupied initially by water. Since the top wall and all side walls of the test cell are insulated, the temperature gradients are approximately zero in the liquid region perpendicular to these boundaries. When the bottom wall temperature was set to a temperature lower than the freezing point, the solidification started from the bottom wall and the phase interface moved upwards over time. In this article, the interface movement will be considered to be one-dimensional.

The position of the phase interface is mainly controlled by time-dependent variations of the bottom wall temperature. The focus of this study is effectively con-

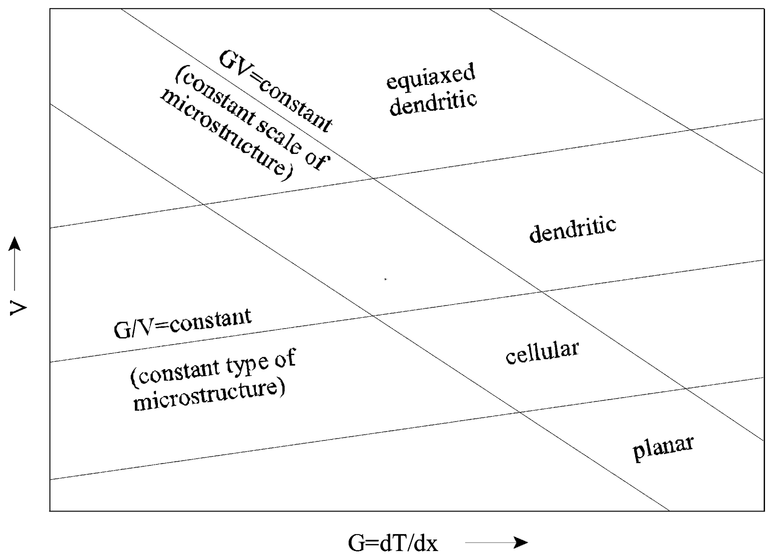

Fig. 1. General schematic of interface structures at varying temperature gradients.

trolling the phase interface motion, as well as the temperature gradient at the phase interface, so that the interface moves upwards at a specified rate after adjusting the bottom wall temperature. Three cases will be considered, i.e., (1) constant cooling temperature (negative interface acceleration), where the phase interface moves slower over time, (2) constant interface velocity (zero acceleration) and (3) constant positive acceleration, so the phase interface moves faster over time.

In general, when a cold temperature is applied to different surfaces of the rectangular test cell, different liquid flow patterns are observed. If a side wall is set as the cold surface, the resulting temperature differences in the liquid can induce natural convection and liquid motion within the test cell. If the top surface is colder than the freezing point, liquid moves downwards due to the density gradients established by the temperature differences therein. With freezing from below, natural convection does not occur during the phase transformation. In that case, heat conduction is the sole mode of energy transfer for the one-dimensional problem. Such conditions are considered in this article, when the bottom wall is cooled and freezing occurs from below. Due to this ice formation, a small gap in the test cell was constructed to accommodate expansion of ice during the phase transition.

The required boundary temperatures were predicted by a numerical inverse method. In the numerical simulation, it is assumed that the interface moves in the y-direction (vertically from the bottom to the top) and the shape of the interface remains planar and horizontal over time. The thermal conductivity, density and specific heat within a particular phase are assumed to be temperature independent. The inverse problem is solved to find how the temperature of the bottom wall should change over time to produce the desired interface motion. The bottom wall temperature is spatially uniform, but it changes over time. These transient changes are predicted by the inverse method, in order to control the phase interface velocity and acceleration during solidification.

The governing equation for diffusion-dominated energy transport with solid/liquid phase change of a pure material can be written as [1]

$$\frac{\partial}{\partial t}(\rho e) = \nabla \cdot (k \nabla T). \tag{1}$$

This equation holds in each phase, while an interfacial heat balance outlines how the interface moves over time. This interfacial heat balance requires that the net heat conducted from the phase interface balances the rate of heat released by phase change at the interface.

In the numerical formulation, an equation of state is needed to write the internal energy, e, in terms of temperature alone. A piecewise linear equation of state is expressed in one equation as follows:

$$e = e_{r,k}(T) + c_{r,k}(T)(T - T_{r,k}), \tag{2}$$

where the subscripts $k = 1, 2$ refer to the solid and liquid phases, respectively. The reference values can be obtained by integration of the Gibbs equation from a point in the liquid phase to another point in the solid phase. In this way, both latent and sensible heat contributions appear in the equation of state.

The reference variables have been consistently set to the following values:

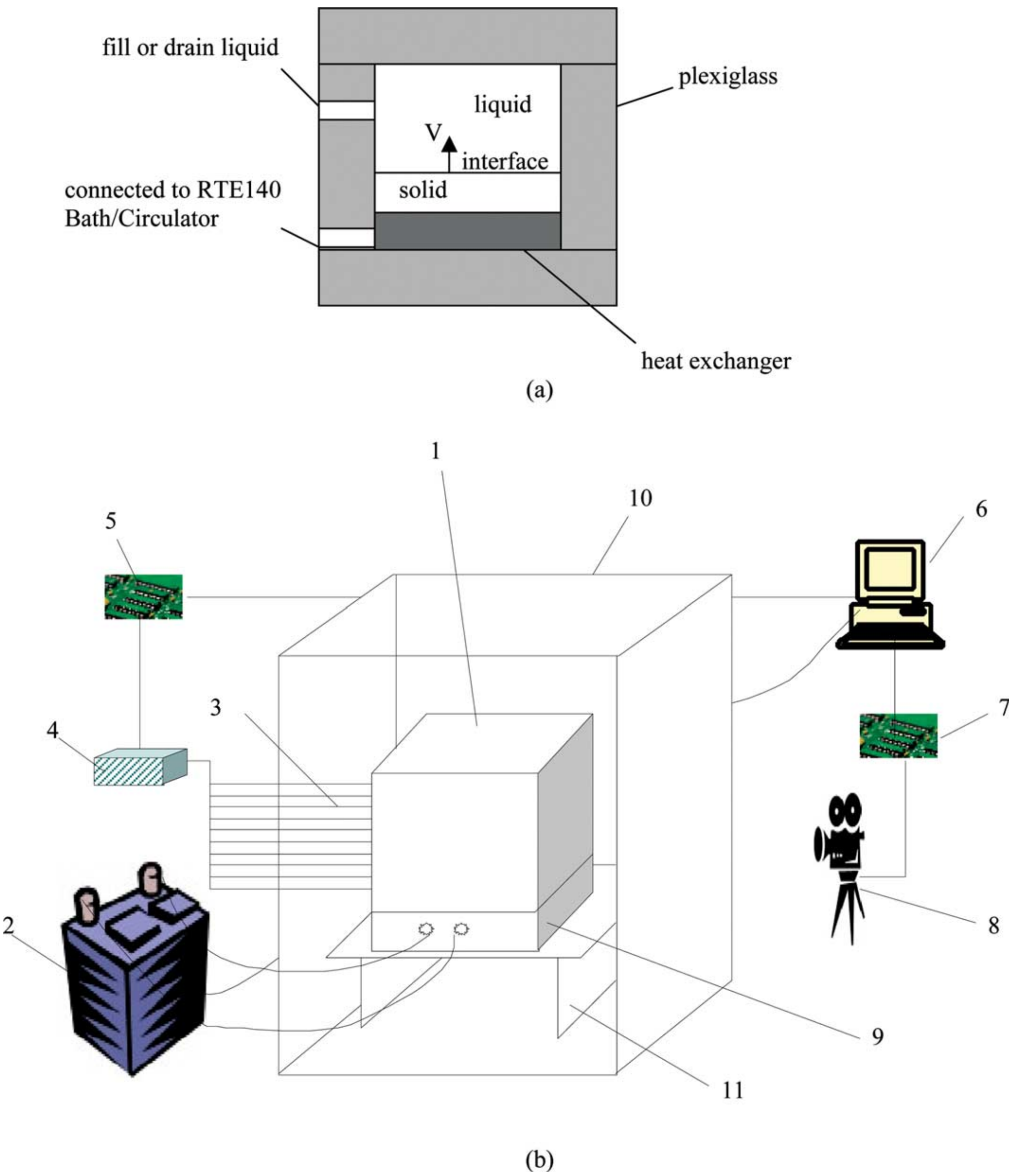

Fig. 2. Schematic of (a) test cell and (b) experimental setup (1. Test Cell, 2. Temperature Bath, 3. Thermocouples, 4. SCB-100 Shielded Connector Block, 5. PCI-6033E DAQ Board, 6. Computer, 7. Image Acquisition Board, 8. Camera, 9. Heat Exchanger, 10. Insulated Enclosure, 11. Support).

($k = 1$, solid phase)

$$e_{r,1} = 0; \quad T_{r,1} = 0; \quad c_{r,1} = \frac{c_s}{c_l}. \tag{3}$$

($k = 2$, liquid phase)

$$e_{r,2} = \frac{\bar{c}}{c_l}(T_l - T_s) + \frac{c_s}{c_l}T_s + \frac{1}{Ste}; \quad T_{r,2} = T_l; \quad c_{r,2} = 1, \tag{4}$$

where $\bar{c} = (c_s + c_l)/2$.

In the inverse formulation, the bottom wall temperature is unknown, while boundary conditions are specified on the remaining surfaces. During each step of the numerical solution, the controlling temperature of the bottom wall is updated iteratively, until the predicted interface movement agrees (within a given tolerance) with the desired interface motion. These iterative updates are predicted based on sensitivity coefficients, which express the influence of boundary temperatures on internal temperatures. As the sensitivity coefficient becomes larger, then the influence of changes of the boundary temperature on an internal nodal temperature becomes stronger. The governing equations are differentiated with respect to the wall temperature, thereby yielding a system of equations involving each nodal sensitivity coefficient. Thus, different sensitivity coefficients are obtained for each nodal point in the mesh. Additional detailed information regarding this inverse method has been documented previously [13–15].

In this article, water is used as the test substance (note: thermophysical properties of water shown in Table 1). The following three cases will be examined.

2.1. Case of constant cooling temperature (negative interface acceleration)

In this first case, the bottom boundary was set at a constant temperature (−10 °C) and a numerical simulation is not needed. The phase interface moves at a high velocity at the beginning of the solidification process, due to a steep initial temperature gradient. As the phase interface moves further from the boundary, it moves slower due to a decreasing temperature gradient. As a result, the phase interface decelerates over time.

2.2. Case of constant velocity (zero interface acceleration)

In this case, the desired condition is interfacial movement at a constant velocity (0.175 mm/min) and zero acceleration. A uniform mesh of 1.75 mm square elements and a constant time step (10 min) were used. The phase interface moves one grid point in each time step, since a node jumping method was used in the numerical simulation. In these simulations, the phase interface moved over a constant distance in each time step.

2.3. Case of constant acceleration (positive interface acceleration)

The desired phase interface motion was specified as follows:

$$y = \frac{1}{2}at^2, \tag{5}$$

where a is a constant positive acceleration. In this case, a non-uniform mesh was generated and a uniform time step was used. At the beginning of the solidification process, the phase interface moves slowly. Then the interfacial velocity increases over time, with a constant acceleration. The phase interface moves faster over time, so it moves over longer distances than previous time steps. In this article, a constant acceleration of 0.00175 mm/min^2 was specified and the time step was 10 min.

Table 1
Thermophysical properties of water

	Value	Units
Specific heat of liquid	4202	J/kg °C
Specific heat of solid	2020	J/kg °C
Thermal conductivity of liquid	0.613	W/m °C
Thermal conductivity of solid	2.26	W/m °C
Density	999.84	kg/m^3
Latent heat	335,000	J/kg
Freezing temperature	0	°C
Liquid thermal diffusivity	1.459×10^{-7}	m^2/s
Solid thermal diffusivity	1.119×10^{-6}	m^2/s

3. Experimental design

In this section, the experimental apparatus, thermocouple temperature measurements, communication with the RTE140 thermal bath and experimental procedure will be described.

3.1. Experimental apparatus

A rectangular test cell was used for the solidification experiments (see Fig. 2a). The test cell has inside dimensions of 6.5 cm (width), 4 cm (height), and 4 cm (depth). The top, bottom, and side walls were made of Plexiglass. All Plexiglass walls were 1.75 cm thick walls to support the cell and provide sufficient insulation. The bottom wall served as the heat sink. It consisted of a multi-pass heat exchanger machined from an aluminum plate. The heat exchanger surface was plated with a layer of chromium for protection against corrosion. A hole on the left surface of the test cell was used to fill or drain liquid. After the initial setup of each experiment, the hole was closed once the container was filled.

Fig. 2b shows a schematic diagram of the test apparatus. For additional insulation purposes, the test cell was placed in the middle of a secondary enclosure. This enclosure was also constructed from Plexiglass, in order that the solidification process remains visible from the front side. The heat exchanger was connected to a NESLAB temperature bath (RTE140 Bath/Circulator). This refrigerated bath can adjust temperatures of the bottom wall to the required temperatures by circulating liquid within the heat exchanger. The thermal bath was connected to the computer through a serial port for communication purposes. A camera was set in front of the test cell for capturing images of the solidification processes. Then, these results were analyzed by a image acquisition system, with feedback signals back to the thermal bath unit.

3.2. Thermocouple temperature measurement system

Ten T-type thermocouples were installed on the back surface of the test cell, along the centerline in the

y-direction. The first thermocouple was located on the bottom surface. All of the other nine thermocouples were placed vertically at intervals of 4 mm. For one-dimensional heat conduction, the effects of 10 thermocouple tips on measured temperatures were considered to be negligible. All of the thermocouples were connected to an SCB-100 Shielded Connector Block, and then assembled to a PCI-6033E DAQ board connected to the computer for temperature measurements. The camera was connected to an image acquisition board attached to the computer to record images.

A PC-based system was developed for the temperature measurements. The system consists of a computer with a plug-in PCI-6033E DAQ board and an SCB-100 Shielded Connector Block. This system was controlled by a LabVIEW program. The thermocouples were connected to an SCB-100 Connector Box. There was a build-on temperature sensor on the SCB-100 board for cold-junction compensation. A differential connection mode was selected with 32 channels. The SCB-100 Connector Box was connected directly to the data acquisition board, which converts analog data to digital data. Thermocouples were monitored with a PC-based data acquisition system (see Fig. 3). The software in the LabVIEW system performs Cold-Junction Compensation, data linearization and control of the time interval between two temperature readings. Also, a Visual Interface (VI) program records each temperature at different locations, after receiving the thermocouple data and writing temperature data to a file. Measurement uncertainties due to thermocouple errors, placement of thermocouples and other uncertainties were estimated to give an overall temperature measurement error of ±0.5 °C.

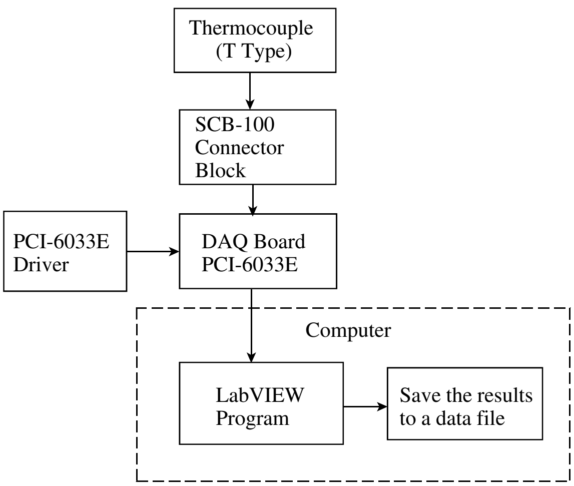

Fig. 3. Components of data retrieval system.

3.3. Communication with RTE140 circulator

A NESLAB-RTE140 Bath/Circulator was used to adjust the bottom wall temperature of the heat exchanger, in order to set the boundary temperatures predicted by the inverse numerical simulation. The circulating fluid was selected to be a 50/50 mixture (by volume) of tap water and laboratory grade ethylene glycol. The operating temperature range was +8 to −30 °C and temperature accuracy of the thermal bath was ±0.05 °C.

Serial communication is used for communication between the RTE140 Bath/Circulator and the computer. This is a common protocol for device communication, which is standard on almost all personal computers. The serial port sends and receives bytes of information, one bit at a time. During transmission, the serial device driver program on the computer takes each byte from the main computer memory (typically 8 KB in size) and places it onto the data bus along with the serial port I/O address. Then, the byte travels through the data bus and it is stored in the serial port hardware buffer. When the serial port is ready to transmit temperature data, it receives the data from this hardware buffer, places it in its shift register, and transmits each bit over the communication line. Serial communication is commonly used because most computers have one or more serial ports, so no extra hardware is needed other than a cable to connect the instrument to a computer. The RTE140 Bath/Circulator has an RS-232 port on its back side. This RS-232 port was used for point-to-point connections between the PC serial ports and the RTE140 Bath/Circulator. This serial communication involved feedback signals from the image acquisition system to the thermal bath during the heat transfer experiments.

A program in LabVIEW was developed to control the RTE140 Circulator. The program sends the instrument command to the RTE140 Circulator via serial port, cable and RS-232 port to the RTE140 Bath/Circulator. Virtual Instrument Software Architecture (VISA) was provided as a single interface library for controlling VXI, GPIB, RS-232 and other instruments in the LabVIEW environment. Some VISA functions were used, such as "VISA Write" and "VISA Read". "VISA Write" sends the setpoints to the RTE140 Bath/Circulator and "VISA Read" receives actual temperatures from the RTE140 Bath/Circulator. The "Read a File" and "Write a File" functions were used for file input/output.

When trying to communicate with the heat exchange devices by serial communication, the serial port sent output as programmed. This requires an exact sequence of code, including termination characters, in order to ensure that the device operates properly. The instrument's termination character for the RTE140 Bath/

Circulator is a carriage return (CR). All commands (including "SS010.00[CR]", i.e., set the setpoint to 10.0 °C) were imported from a file, so it was difficult to add a CR alone as a termination character in a text file. Text editors usually add a CR and a line feed automatically, whenever the "Enter" key is hit on a computer's keyboard. As a result, a "Concatenate Strings" function was used to append a CR constant to the string before it was sent to the serial port. The CR constant from the Strings function palette in LabVIEW was used.

The LabVIEW VI program can perform serial communication between the RTE140 Bath/Circulator and computer. The required setpoint for the RTE140 Bath/Circulator was edited in a text file. The VI program opened the file and converted it to an exact command format as required by the RTE140 Bath/Circulator. A termination character was added by a CR to the end of the string. It reads the commands from the file and sends the commands to the RTE140 Bath/Circulator. Then, the RTE140 Bath/Circulator follows the commands sent. Meanwhile, the program reads actual temperatures from the RTE140 Bath/Circulator and writes them to a file.

3.4. Experimental procedure

Before each experiment, the phase interface movement was specified for each case. The results of each experiment require that the phase interface moves upwards as specified. The numerical results were used as the required boundary temperatures, in order to obtain those desired phase interface movements. The required boundary temperature results of the inverse numerical simulation were saved in a data file. This data was used as input to adjust the setpoints of the temperature bath by serial communication. As described earlier, a fluid was circulated at the setpoint temperature within the heat exchanger, which was located under the bottom wall of the test cell. In this way, the bottom surface temperatures were controlled over time, in order to produce the desired phase interface motion.

Before an experiment started, the test cell was filled with water, except a small gap left for expansion of freezing water. The setpoint of the temperature bath was set to the freezing point of 0.0 °C, so only liquid existed initially. This initial condition was established for a few hours, in order to obtain a uniform temperature distribution within the test cell. Fig. 4 shows a diagram of the experimental procedure. The LabVIEW program included a sub-program for serial communication, thermocouple measurements and image acquisition (interface detection program). These three sub-programs were placed into a "While" loop, so they can be repeated at a certain time interval. After the experiment starts, the algorithm sends the setpoints of the thermal bath and reads back actual temperatures by serial communication. In the meantime, the computer records and saves temperature measurements in a file. Also, the camera

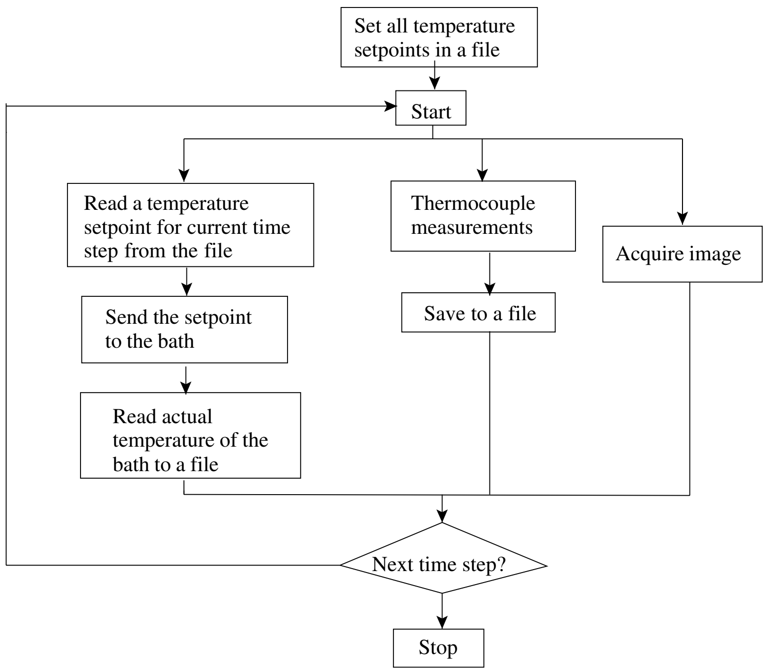

Fig. 4. Schematic of experimental procedure.

captures images of the interface movement. The image acquisition system analyses this data, records the interface position and sends feedback signals to the thermal bath. This procedure is repeated every few minutes, thereby providing thermal control of the interface motion.

4. Results and discussion

In this section, the following three cases of water/ice solidification will be studied: (1) constant cooling temperature (negative interface acceleration), (2) constant velocity (zero acceleration) and (3) constant positive acceleration of the phase interface. The required boundary temperatures predicted by the inverse numerical simulation are shown in Fig. 5. Fig. 5 illustrates how the required boundary temperatures vary with time for the three cases, in order to produce the desired interfacial movements. For case (1), the boundary temperature is constant. For case (2) with a constant interfacial velocity, a lower boundary temperature is required when the phase interface is further from the boundary. For case (3), the required boundary temperature decreases slowly when the interface is close to the bottom wall. As the interface moves further away from the bottom wall, the required boundary temperature decreases faster.

The required boundary temperatures were applied to establish the setpoints of the temperature bath, in order to make the bottom wall temperature vary with time as required. During the experiments, the setpoint of the temperature bath was kept constant at each time step. The temperatures of the thermal bath were measured to confirm whether the actual temperatures of the control system followed the setpoints. Fig. 6 shows a comparison between the setpoints and actual temperatures of the

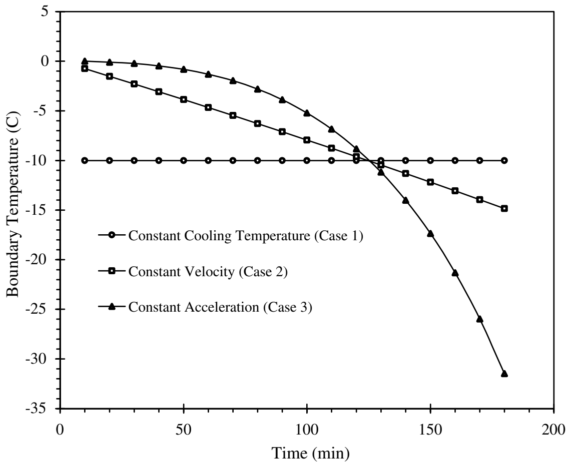

Fig. 5. Predicted boundary temperature.

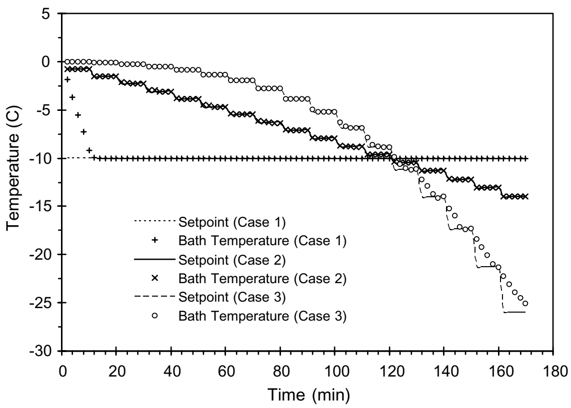

Fig. 6. Bath temperature and setpoint for case 1 (constant cooling temperature), case 2 (constant velocity) and case 3 (constant acceleration).

thermal bath for the three cases. It can be seen that the temperature bath needed a certain time period to respond after the setpoint was changed. This time period depended on the setpoint temperature. When this temperature was not too low, the thermal bath required about a few minutes to reach the setpoint. When the temperature setpoint was further lowered, the thermal bath needed more time to cool down and reach the setpoint.

For the constant cooling temperature case, the bath temperature was set to −10 °C. The temperature bath cannot cool down to that temperature immediately due to thermal inertia, as it needs a certain amount of time to reach that temperature. Once the temperature reached −10 °C, it was kept at that temperature in a stable manner. For the constant velocity case, the bath temperature followed the setpoints well. For the constant acceleration case at early time steps, the actual temperature also matched the setpoints well. But as the temperature of the control system becomes low at later times, a longer time period was needed for cooling by a fixed amount. The temperature of the thermal bath did not follow the setpoints well at later times, especially when the setpoint becomes lower than −20 °C. This problem is considered to be related to the cooling capacity of the refrigerated bath. A larger capacity would reduce or eliminate this problem, depending on the desired range of experimental conditions.

Fig. 7 shows the temperature variations at each thermocouple location for the three cases. Supercooling of water was observed from the temperature measurements, before freezing of water began. The solidification did not start immediately at the freezing temperature, but rather it started at a few degrees lower than the freezing point. At the beginning of an experiment, the temperatures of the bottom wall were kept below the

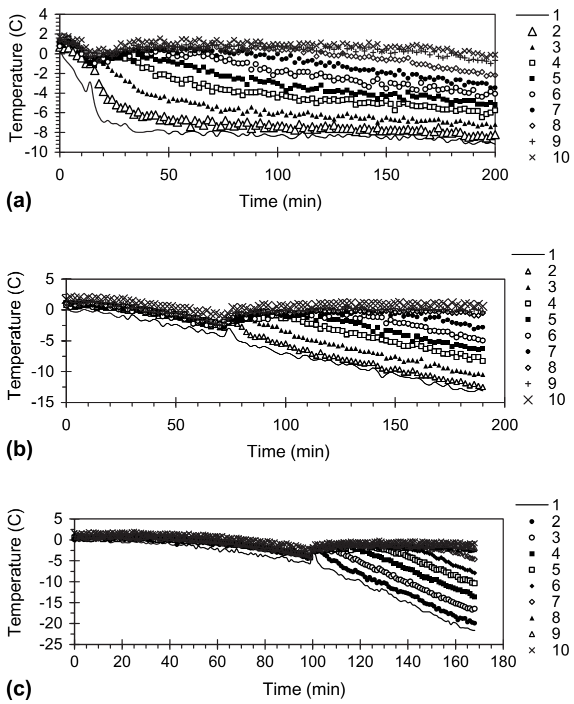

Fig. 7. Measured temperatures for (a) case 1, (b) case 2 and (c) case 3.

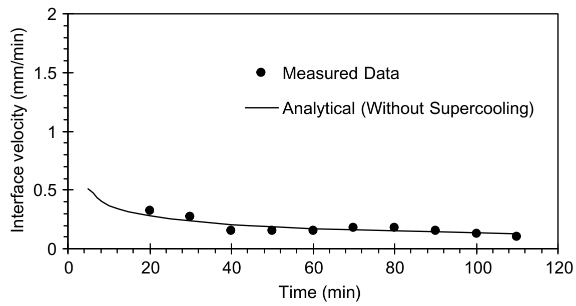

Fig. 8. Interface velocity (case 1: constant cooling temperature).

freezing point and temperatures at all thermocouple locations decreased. When the water was supercooled by a certain extent, ice growth started from a nucleation site on the wall and latent heat was released in the freezing process. Nucleated crystals in the bulk liquid were not observed.

Thermocouple measurements for each case are shown in Fig. 7. The 10 thermocouples were spaced uniformly in the y-direction along the vertical centerline of the test cell. Thermal recalescence can be observed in Fig. 7. After the temperatures at all thermocouple locations approached a certain sub-zero point, they appeared to increase abruptly over a short time period, despite cooling by the bottom wall. Latent heat was released from the solidified crystals, which was transferred by conduction to the surrounding solid or liquid. The local temperature rises, if the rate of release of latent heat exceeds the rate at which heat is removed from the solidifying material and cooling boundary. After the short time period of recalescence, the temperatures decreased again due to continued cooling from the bottom wall. After ice initially appears on the wall, the remaining water changes phase at 0 °C. Before this phase change, it was noticed that the degree of supercooling below the freezing point was different for each case. The supercooling was −0.98 °C for the constant cooling temperature case, −2.7 °C for the constant velocity case and −3.8 °C for the constant acceleration case. These differences were related to the nucleation kinetics and different rates of initial water cooling near the bottom wall.

For case 1 in Fig. 8, the measured interface velocity is obtained from differencing of measured interface positions over time. It can be seen that the phase interface moves faster when the interfacial position is closer to the boundary. When this interface is further away, it moves slower since heat is conducted through a thicker solid layer before it is transferred across the chilled boundary. The interface decelerates non-linearly with time, since the phase interface moves at a non-uniform velocity. Therefore, if a constant phase interface velocity is expected during solidification, the boundary temperature must vary with time.

In the constant velocity case (zero interface acceleration), Fig. 9a illustrates how the phase interface position varies with time. A comparison of measured and desired interface positions shows generally good agreement (note: period of "delay" corresponds to supercooling period). At early stages of solidification, the measured and desired phase interface positions matched closely. But the measured interface position deviated from the desired position at later stages of solidification, when the phase interface moved slightly slower than desired.

In the constant acceleration case (Fig. 9b), it can be seen that there was a long time period of supercooling and the measured interface position was delayed, when compared to the desired position. However, after the period of supercooling, the interface moved faster and its rate of advance agreed well with the desired motion. Supercooling of water is a source of error, since some time elapses before solidification is initiated at the wall. This error can be addressed by a time delay corresponding to the unfrozen period. In Fig. 9a and b, the phase interface positions do not match the desired interface positions, without such "delay". However,

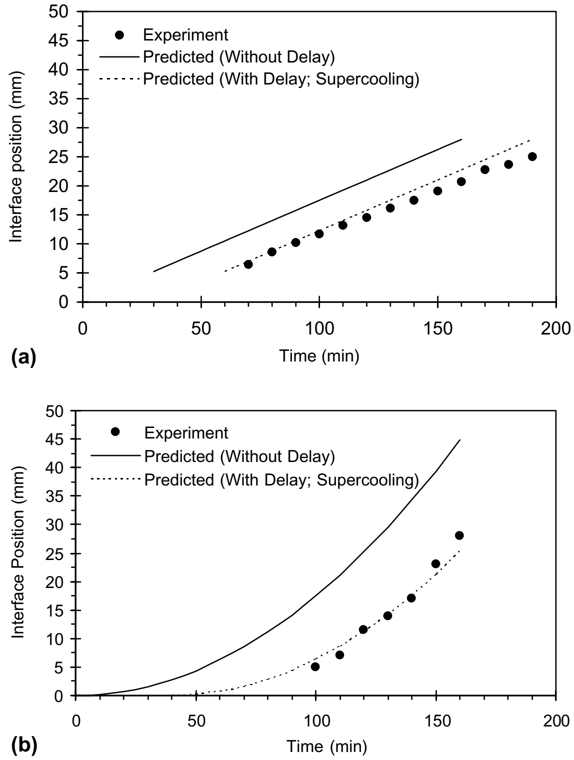

Fig. 9. Interface movement for (a) case 2 and (b) case 3.

with appropriate time steps of delay due to supercooling, the agreement between measured and predicted interface positions becomes reasonably good. These time steps can be predicted from an analytical solution to reach the sub-zero supercooled point [1]. The predicted results with a delay represent the desired phase interface position. Both results with and without this delay have nearly the same slope. This slope represents the velocity of the phase interface.

Fig. 10 shows how the interfacial temperature gradients on the liquid side of the phase interface varied with time for the three cases. These spatial gradients are determined from a polynomial profile fitted to measured temperatures at the interface, together with the known interface temperature and its measured position. The overall trends indicate that the interfacial temperature gradients decreased, remained constant and increased over time for cases 1–3, respectively. With zero acceleration of the phase interface (case 2), the rate of heat transfer by conduction on both sides of the interface remains constant in the interfacial heat balance, as the heat balance requires a constant rate of latent heat released from the interface. Conversely, the heat conduction rates change over time when the interface is accelerated, so the results indicate the proper trend of rising interfacial temperature gradients in case 3 (note:

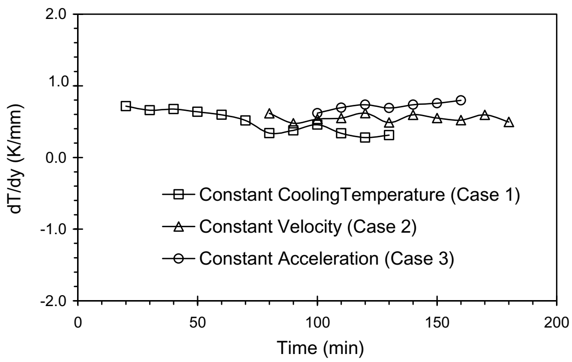

Fig. 10. Temperature gradients at the phase interface.

decelerating interface in case 1 with decreasing interfacial temperature gradient).

In Fig. 10, the three cases have different trends of temperature gradient at the phase interface. Such variations have certain effects on the microstructure of solidified ice. Fig. 11 shows two images of ice formed during two different solidification processes. Fig. 11a and b show the constant cooling temperature (case 1) and constant velocity case (case 2), respectively. It appears that ice solidified differently in both cases. In Fig. 11a, the lower part of the image is white, since ice

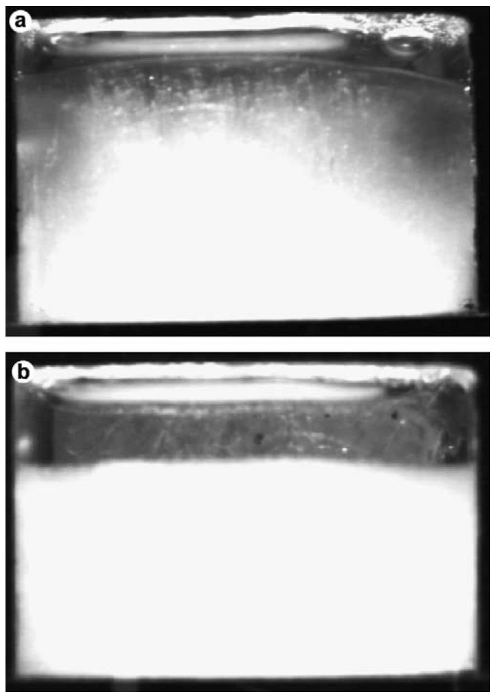

Fig. 11. Photographs of ice formation for (a) case 1 and (b) case 2.

forming in the lower section was not transparent. The higher region of the image is darker, since that ice formation was more transparent. The darker color suggests that the ice was more transparent, since there was a black background behind the test cell. The ice microstructure is affected by the interfacial acceleration and temperature gradients. Ice formation at a constant phase interface velocity had a nearly constant interfacial temperature gradient. In Fig. 11, ice formation during this process would seem to have the same microstructure. This may explain why the ice accumulated differently in the constant cooling temperature case, yet identically in the constant velocity case.

Efforts were taken to minimize experimental errors and uncertainties as much as possible. For example, when the fluid circulated between the temperature bath and the heat exchanger, some heat losses may have occurred. A plastic tube with insulation was made as short as possible to connect the temperature bath and heat exchanger. Heat losses from the test cell were minimized by extensive insulation of the test cell. Reported temperatures were estimated to be accurate within ±0.5 °C. At each time step, when the setpoint was adjusted, the temperature of the thermal bath could not reach that temperature immediately. Thus, there was a delay (depending on the size of temperature difference adjusted, usually up to a few minutes). At some time steps, the temperature of the thermal bath had not reached the setpoint during that time step. This effect could be reduced with a thermal bath of larger thermal capacity.

5. Conclusions

In this article, one-dimensional freezing of water and interface motion have been successfully controlled with a newly developed numerical/experimental algorithm. The required boundary temperature was predicted based on an inverse numerical simulation. It was used to control the interfacial velocity, acceleration and temperature gradients. Solidification experiments involving water were performed in a rectangular test cell. The automated system controlled the temperature at the bottom wall, while circulating liquid within a heat exchanger embedded within that wall. Three cases were performed, including a constant wall temperature (negative interface acceleration), constant velocity (zero acceleration) and constant positive acceleration of the phase interface. The experimental results have shown that interfacial acceleration affects the interfacial temperature gradients. Varying interface movements and temperature gradients lead to different solidified material structures. Also, supercooling has noticeable effects on the thermal control of phase interface motion. In conjunction with other control strategies such as closed-loop feedback control, it is anticipated that the newly developed method can provide better results to compensate for supercooling effects and other errors during a controlled solidification process.

Acknowledgements

Financial support from the Natural Sciences and Engineering Research Council of Canada and a University of Manitoba Graduate Fellowship (R. Xu) for this research are gratefully acknowledged.

References

[1] G.F. Naterer, Heat Transfer in Single and Multiphase Systems, CRC Press, Boca Raton, FL, 2002 (Chapters 5 and 8).
[2] N. Zabaras, Y. Ruan, O. Richmond, Design of two-dimensional Stefan processes with desired freezing front motions, Numer. Heat Transfer B 21 (1992) 307–325.
[3] N. Zabaras, K. Yuan, Dynamic programming approach to the inverse Stefan design problem, Numer. Heat Transfer B 26 (1994) 97–104.
[4] J.I. Frankel, M. Keyhani, A new approach for solving the inverse solidification design problem, Numer. Heat Transfer B 30 (2) (1996) 161–177.
[5] S.W. Hale, M. Keyhani, J.I. Frankel, Design and control of interfacial temperature gradients in solidification, Int. J. Heat Mass Transfer 43 (2000) 3795–3810.
[6] H.H. Demirci, J.P. Coulter, S.I. Guceri, A numerical and experimental investigation of neural network based intelligent control of molding processes, ASME J. Manufact. Sci. Eng. 119 (1997) 88–94.
[7] J. Alkemper, S. Sous, C. Stocker, L. Ratke, Directional solidification in an aerogel furnace with high resolution optical temperature measurements, J. Cryst. Growth 191 (1998) 252–260.
[8] G.E. Schneider, M. Raw, An implicit solution procedure for finite difference modeling of the Stefan problem, AIAA J. 22 (1984) 1685–1690.
[9] D.R. Poirier, Permeability for flow of interdendritic liquid in columnar-dendritic alloys, Metall. Trans. B 18 (1987) 245–255.
[10] G.F. Naterer, Establishing heat-entropy analogies for interface tracking in phase change heat transfer with fluid flow, Int. J. Heat Mass Transfer 44 (15) (2001) 2903–2916.
[11] G.F. Naterer, J.A. Camberos, Entropy and the second law in fluid flow and heat transfer simulation, AIAA J. Thermophys. Heat Transfer 17 (3) (2003) 360–371.
[12] C.J. Ho, R. Viskanta, Heat transfer during inward melting in a horizontal tube, Int. J. Heat Mass Transfer 27 (1984) 709–716.
[13] R. Xu, G.F. Naterer, Controlling phase interface motion in inverse heat transfer problems with solidification, AIAA J. Thermophys. Heat Transfer 17 (4) (2003) 488–497.

[14] R. Xu, G.F. Naterer, Inverse method with heat and entropy transport in solidification processing of materials, J. Mater. Process. Technol. 112 (2001) 98–108.

[15] R. Xu, Control of heat and fluid flow in solidification processes by an inverse method, M.Sc. Eng. Thesis, Lakehead University, Thunder Bay, Canada, 1999.